REPORT DOCUMENTATION PAGE

Form Approved
OMB No. 0704-0188

1. REPORT DATE	2. REPORT TYPE	3. DATES COVERED
	Professional Paper	

4. TITLE AND SUBTITLE	5a. CONTRACT NUMBER
Modulated Laser Line Scanner for Enhanced Underwater Imaging	5b. GRANT NUMBER
	5c. PROGRAM ELEMENT NUMBER

6. AUTHOR(S)	5d. PROJECT NUMBER
Linda Mullen; Michael Contarion; Brian Concannon; Jon Davis	5e. TASK NUMBER
	5f. WORK UNIT NUMBER

7. PERFORMING ORGANIZATION NAME(S) AND ADDRESS(ES)	8. PERFORMING ORGANIZATION REPORT NUMBER
Naval Air Warfare Center Aircraft Division 22347 Cedar Point Road, Unit #6 Patuxent River, Maryland 20670-1161	

9. SPONSORING/MONITORING AGENCY NAME(S) AND ADDRESS(ES)	10. SPONSOR/MONITOR'S ACRONYM(S)
Naval Air Systems Command 47123 Buse Road Unit IPT Patuxent River, Maryland 20670-1547	11. SPONSOR/MONITOR'S REPORT NUMBER(S)

12. DISTRIBUTION/AVAILABILITY STATEMENT

Approved for public release; distribution is unlimited.

13. SUPPLEMENTARY NOTES

14. ABSTRACT

Current Laser Line Scanner (LLS) sensor performance is limited in turbid water and in bright solar background conditions. In turbid water, backscattered and small angle forward scattered light reaching the receiver decreases underwater target contrast and resolution. Scattered solar energy reaching the detector also decreases detection sensitivity by increasing receiver noise. Thus, a technique which rejects unwanted, scattered light while retaining image-bearing photons is needed to improve modulation and detection techniques to the LLS. This configuration will enable us to use optical modulation to discriminate against scattered light. A nonscanning mockup of an existing LLS, the Electro-Optic Identification (EOID) sensor, has been developed with off-the-shelf components. An electro-optic modulator will be added to this systm to crate a modulated LLS prototype. Laboratory tank experiments will be conducted to evaluate the performance of the modulated LLS as a function of water clarity and solar background levels. The new system will be compared to its unmodulated counterpart in terms of target contrast.

15. SUBJECT TERMS
lidar, underwater imaging, optical modulation, laser line scanner

16. SECURITY CLASSIFICATION OF:			17. LIMITATION OF ABSTRACT	18. NUMBER OF PAGES	19a. NAME OF RESPONSIBLE PERSON
a. REPORT	b. ABSTRACT	c. THIS PAGE			19b. TELEPHONE NUMBER (include area code)
Unclassified	Unclassified	Unclassified	Unclassified	8	Linda Mullen (301) 342-2021

Modulated Laser Line Scanner for Enhanced Underwater Imaging

Linda Mullen[a], V. Michael Contarino[a], Alan Laux[a], Brian Concannon[a], Jon Davis[a], Michael Strand[b], Bryan Coles[c]

[a]Naval Air Warfare Center Aircraft Division, Patuxent River, MD 20670

[b]Naval Surface Warfare Center, Panama City, FL 32407

[c]Raytheon Company, Tewksbury, MA 01876

ABSTRACT

Current Laser Line Scanner (LLS) sensor performance is limited in turbid water and in bright solar background conditions. In turbid water, backscattered and small angle forward scattered light reaching the receiver decreases underwater target contrast and resolution. Scattered solar energy reaching the detector also decreases detection sensitivity by increasing receiver noise. Thus, a technique which rejects unwanted, scattered light while retaining image-bearing photons is needed to improve underwater object detection and identification. The approach which we are investigating is the application of radar modulation and detection techniques to the LLS. This configuration will enable us to use optical modulation to discriminate against scattered light. A nonscanning mock-up of an existing LLS, the Electro-Optic Identification (EOID) sensor, has been developed with off-the-shelf components. An electro-optic modulator will be added to this system to create a modulated LLS prototype. Laboratory tank experiments will be conducted to evaluate the performance of the modulated LLS as a function of water clarity and solar background levels. The new system will be compared to its unmodulated counterpart in terms of target contrast.

Keywords: lidar, underwater imaging, optical modulation, laser line scanner

1. INTRODUCTION

The ability to image objects underwater is limited by several physical processes which occur as light propagates through water. Light traveling underwater from an optical source to a distant receiver is attenuated by absorption (loss of photons) and scattering (photons scattered out of the field of view of the receiver) by water particulates and dissolved substances. The ultimate limit to the range at which an underwater object can be detected is determined by this attenuation. Before the photon limit is reached, image contrast and resolution can be degraded by optical scattering in several ways. Some light which does not reach the underwater object is reflected by water particles and biological organisms into the receiver field of view. This backscattered light creates a background noise level which degrades the image contrast. Secondly, light which reaches and is reflected from an underwater target encounters small forward angle scattering on its travel to the receiver. This scattering degrades contrast by decreasing the image sharpness or resolution. Finally, scattered light originating from other optical sources, such as the sun, can also increase the detector noise level at shallow depths.

Unlike photon limited detection, contrast limited detection cannot be improved simply by increasing the transmitted optical power (or the detector quantum efficiency). However, a method for separating the unscattered (or minimally scattered), image bearing photons from the multiply scattered, background light could be used to improve object detection and imaging. Several systems have been developed to accomplish this task. The laser line scan system uses a well collimated continuous wave laser source and a narrow field of view receiver to spatially separate scattered and unscattered light. In this system, the bistatic source and receiver are aligned to intersect at a distant plane of interest. This configuration reduces backscatter since the common volume between the source and receiver is limited. The forward scatter problem is decreased by the narrow field of view, and high spatial resolution is achieved by the narrow diameter illuminating beam. High quality images have been produced with single[1] and multiple[2] channel receivers.

The LLS characteristics which enable the system to collect impressive underwater images also lead to certain limitations. Since the system uses a continuous wave source, no inherent time (depth) information is present in the detected signal, and

post-processing using triangulation methods must be used to obtain three dimensional images. Furthermore, the use of a continuous wave source increases the receiver integration time which can limit system performance in shallow water, high solar background environments. Finally, in very turbid water, the effects of multiple scattering can degrade image contrast and resolution and limit the detection range.

In the next section, a new approach for underwater imaging is described. The hybrid lidar-radar technology uses optical modulation to reduce background noise and enhance underwater target contrast. The application of this technology to the LLS is discussed.

2. HYBRID LIDAR-RADAR

The hybrid lidar-radar detection scheme was developed to improve backscatter rejection and image sharpness or resolution in a scattering environment, such as ocean water[3,4]. As shown in Figure 1, the hybrid lidar-radar system is formed when a microwave subcarrier is superimposed on an optical carrier, is transported through the scattering medium via the optical signal, and is recovered by a high speed optical detector and a microwave receiver. This system enables one to use microwave radar to perform target detection and ranging in situations where microwaves cannot be used directly (i.e., in ocean water). The hybrid lidar-radar system benefits from the transmission characteristics of the optical carrier (lidar) and the coherent detection and signal processing techniques possible with the lower frequency microwave subcarrier (radar).

The basic approach of the hybrid lidar-radar detection scheme is to make use of the way in which each component of the return signal is affected by the scattering of the modulated optical signal. Since the backscatter signal arises from reflections from a volume of randomly distributed scatterers, the modulation is essentially 'washed out' in this signal component. Light which is reflected from an underwater object and is multiply scattered on its travel back to the receiver is also demodulated relative to the minimally scattered, image-bearing light. By filtering the return signal at the subcarrier modulation frequency, this technique provides a method of rejecting the demodulated, scattered light while retaining the coherent, unscattered (or minimally scattered) modulated signal. This rejection of scattered light can also help reduce solar ambient noise. When coherent detection schemes are used, the short wavelength of the microwave subcarrier can also provide accurate depth information.

Since optical scattering in turbid water and high solar background environments currently limits LLS performance, the application of the hybrid lidar-radar approach to the LLS system is a possible solution for improving underwater detection. The subcarrier modulation can potentially benefit the LLS system in several ways: 1) improve image contrast by reducing backscatter; 2) decrease solar ambient noise; and 3) enhance image sharpness by decreasing forward blur/glow scatter. The short wavelength of the microwave subcarrier can also provide accurate depth information when coherent detection schemes are used.

The remainder of this paper will describe a modulated LLS prototype which was designed within the specifications of an existing LLS, the Electro-optic Identification sensor (EOID). Laboratory experiments were conducted to assess the ability of the modulated system to reduce backscatter and solar ambient noise and to improve underwater target contrast. Results from these experiments will be discussed.

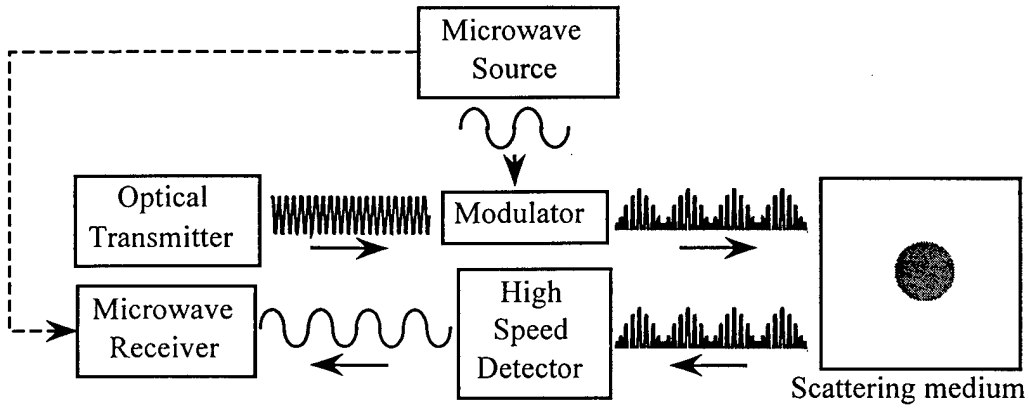

Figure 1. Hybrid lidar-radar block diagram. The microwave subcarrier is encoded on the optical carrier and is recovered by a high speed detector and microwave receiver.

3. MODULATED LLS PROTOTYPE

The following paragraphs will describe the major components of the experimental setup: the modulated optical transmitter, the optical receiver and signal analyzer, and the water tank facility. The prototype was designed so that several issues could be addressed in the experiments, including the dynamic range of the photodetector and the effect of modulation frequency, water clarity, and solar background level on the system performance. A diagram of the complete setup is shown in Figure 2.

3.1. Modulated optical transmitter

The Laser Power microlaser was chosen for its 532 nm, high output power (1.5 watts polarized) and its compact, energy efficient packaging. The high power is needed since the average optical power is reduced by 50% by modulating the transmitted beam. Since the current EOID sensor operates with a 500 mw laser, this optical power is sufficient to compare with the existing system.

A wide band electro-optic modulator with high optical power handling capabilities, good linearity, and high modulation index was chosen to modulate the laser output. The range of modulation frequencies was limited by the current EOID specifications. The lower limit was set by the inverse of the integration time per pixel which ranges from 33kHz-300kHz. A factor of ten was added to this range to insure a sufficient number of modulation cycles in each pixel (330kHz-3MHz). The upper limit is fixed by the photodetector bandwidth which was measured to be approximately 90MHz. Three frequencies were chosen for the measurements: 10MHz, 50MHz, and 90MHz. The modulation source was provided by the network analyzer which was also used as the signal analyzer.

3.2. Optical receiver and signal analyzer

The main issue in the design of the optical receiver was to insure that there was sufficient dynamic range to detect the high solar background levels and the modulated optical signal. The current EOID sensor has an eight stage photomultiplier tube (PMT) with a resistive voltage divider, a gain ranging from 400 to 32E4, and a bialkali photocathode. To increase the linearity range, a seven stage, active voltage divider was used. By individually biasing each of the dynodes with a variable power supply, the dynode voltages remained stable even at high output currents and the voltage distribution could be easily modified. In addition, a PMT with a lower resistivity S20 photocathode was used. The PMT sensitivity was measured with a gain of 4.5E4 and remained linear up to 5 ma of anode current. The effect of the DC current on the PMT bandwidth was also measured by keeping the modulated optical input at a constant level while the DC light level was increased. As expected, the bandwidth began to decrease when the tube response became nonlinear. The tube remained in the linear operating region throughout the range of experiments.

In concurrence with the EOID sensor configuration, a 2", f2.5 lens was placed in front of the PMT. A variable aperture at the lens focal point controlled the field of view (FOV) which ranged from 0.75 degrees (current EOID FOV) to 4 degrees. A bias tee was connected to the output of the PMT so that both the DC current (LLS) and the AC modulation (modulated LLS) could be measured separately. A network analyzer was used to monitor the modulated signal power. Since the network analyzer was also used to drive the optical modulator, the difference in phase between the transmitted and detected modulated optical signals was measured. This was converted into target range for each of the modulation frequencies used in the experiments.

3.3. Water tank facility

The Aqua Tunnel water tank facility at NAWC was used for the laboratory measurements. The tank is 3.7m x 0.9m x 0.9m with 0.6m windows on each end. The tank interior is painted black to decrease internal reflections, and the windows are tilted at an angle to prevent direct reflections from the glass surface. The tank water is continuously circulated to ensure a homogeneous water volume, and an in-line pool filter is used to clean the water after scattering agents have been added. The scattering properties of ocean water were simulated by the addition of Maalox antacid which has been shown to be a good match to the volume scattering function of natural waters[5]. The correlation between Maalox concentration and beam attenuation coefficient was derived from previous AC9 measurements[6]. As shown in Figure 2, the transmitter and receiver were situated at one end of the tank and a target was placed in front of the window on the opposite side of the tank. The target used in the experiments was a diffuse white target (reflectivity ~ 90%) which covered the entire back window. Measurements were also made with black wetsuit material (reflectivity ~ 10%) covering the back window so that a relative target contrast

could be calculated. The transmitter and receiver were aligned to intersect at the middle of the target. The ambient solar background was simulated with two 500W halogen lamps that were situated above the tank.

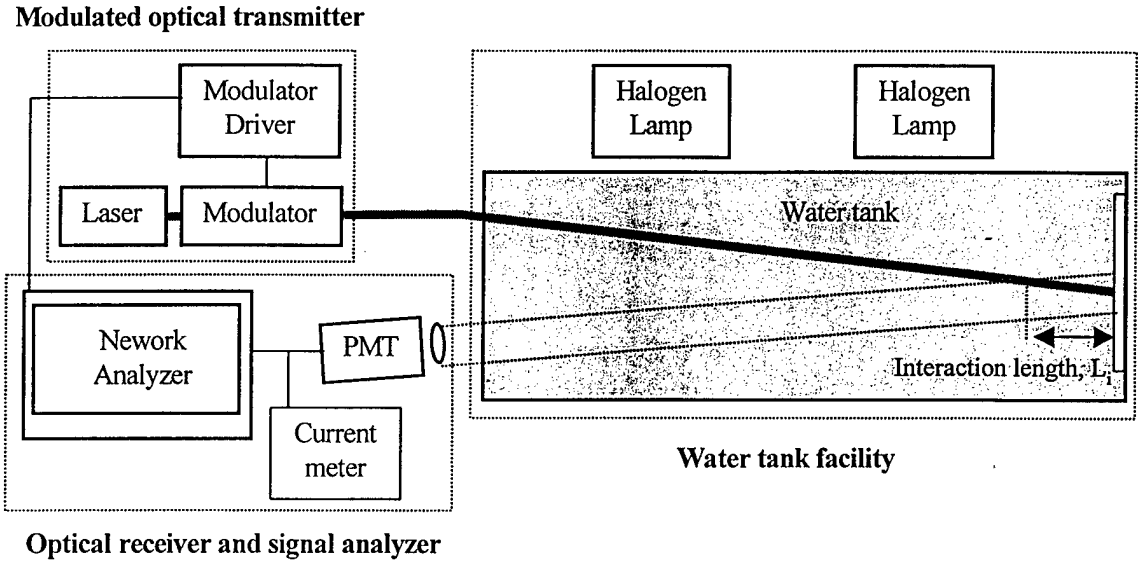

Figure 2. Experimental setup for testing the modulated LLS prototype. The setup includes three major components: the modulated optical transmitter, the optical receiver and signal analyzer, and the water tank facility. The interaction length, L_i, is the distance over which the transmitted beam and receiver field of view overlap.

4. EXPERIMENTAL RESULTS

The purpose of the first set of measurements was to measure the contrast of the white target relative to the black target (wetsuit material) as a function of water clarity and modulation frequency. The contrast was computed by dividing the difference of the white and black target amplitudes, A_{white} and A_{black}, respectively, by the sum of the two, or

$$\text{Contrast} = (A_{white} - A_{black})/(A_{white} + A_{black}). \quad (1)$$

The transmitter-receiver separation was 17 inches and the FOV was 0.75 degrees, which are the current settings for the EOID sensor. For this configuration, the interaction length, L_i, shown in Figure 2 was approximately 1m. This length corresponds to the distance over which the transmitted beam and receiver field of view overlap. The results are shown in Figure 3 where the contrast for the DC (LLS) and the AC (modulated LLS) signal components are plotted as a function of the beam attenuation coefficient. The 10 MHz and DC contrasts overlap throughout the range of water clarities tested. This is due to the fact that the 10 MHz wavelength (30 m) is significantly longer than the roundtrip interaction length, $2L_i$=2m. For backscatter cancellation to occur, pathlength differences on the order of the modulation wavelength must be present. As the modulation wavelength decreased relative to the roundtrip interaction length (for f_m=50MHz, $\lambda_{50MHz}/2L_i$=3; for f_m=90MHz, $\lambda_{90MHz}/2L_i$=1.7), increased cancellation of the backscatter occurred and the target contrast was enhanced. Furthermore, as the number of scattering centers within the transmitter-receiver common volume increased, the backscatter began to dominate the low frequency returns (DC and 10 MHz) while becoming more demodulated at the higher modulation frequencies (50MHz and 90MHz). This trend is evident in Figure 3 for c>0.6 m where the slope of contrast vs. beam attenuation increases as the modulation frequency decreases.

The phase data illustrated the effect of the backscatter on estimating target range. At each Maalox concentration, the measured target phase was converted into distance for each modulation frequency. The results are shown in Figure 4 where the calculated target range is plotted against the beam attenuation coefficient. The dashed line indicates the true target location (3.66 m). The target range calculated from the 10MHz data showed an increasing bias towards shorter depths as the

beam attenuation increased. This is due to the fact that at this modulation frequency, the target return phase was a combination of the target itself and the accumulated backscatter signal. As the water clarity decreased due to increasing particle concentration, the integrated backscatter phase dominated over the target phase and resulted in an incorrect prediction of the true target range. However, at modulation frequencies of 50MHz and 90MHz, the target range error was less than 0.1m for the dirtiest water measured. These results are evidence that the backscatter phase did not contribute significantly to the measured target return phase and a more precise estimation of the true target range is obtained with the higher modulation frequencies.

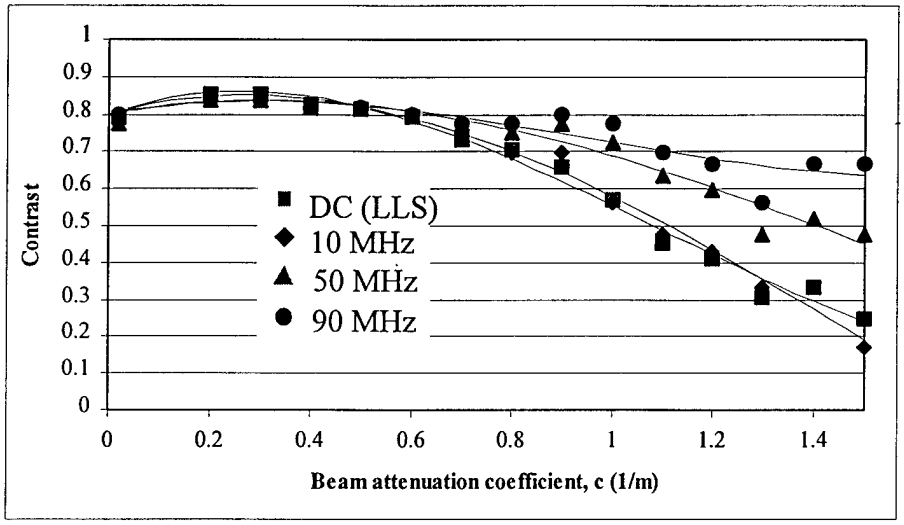

Figure 3. Target contrast as a function of beam attenuation coefficient and modulation frequency. The 50MHz and 90 MHz data show an enhanced target contrast due to backscatter cancellation.

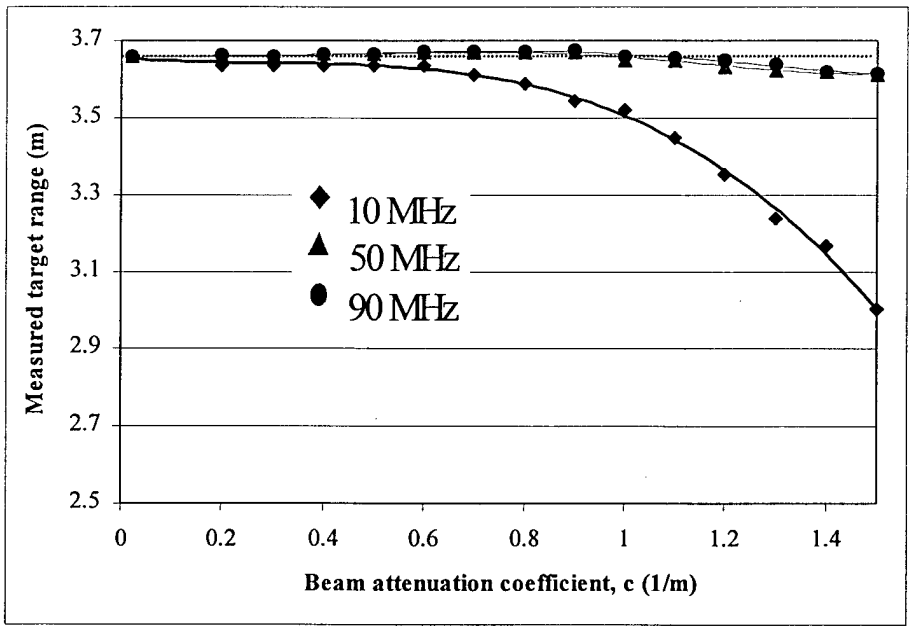

Figure 4. Measured target range as a function of beam attenuation coefficient and modulation frequency. The dashed line indicates the true target range. Although the 10 MHz data shows an increasing bias towards shallower depths, the 50MHz and 90MHz data produce a more accurate estimation of the target range.

In the second set of experiments, the effect of moving the transmitter and receiver closer together and increasing the transmitter-receiver common volume was studied. The transmitter and receiver were moved to a 0.2m separation and were

realigned to intersect at the target center. For this configuration, the interaction length increased to approximately 2m. The results for target contrast are shown in Figure 5. The same trends occurred as with the 0.43m separation: the 10 MHz and DC contrasts overlapped, and the 50MHz and 90MHz data showed an increase in target contrast relative to the lower frequency data. However, the DC and 10 MHz contrasts began to decrease at a lower c value ($0.4m^{-1}$) than the data obtained with a 0.43m separation ($c=0.5m^{-1}$). This was due to the increased common volume between the transmitter and receiver and corresponding increase in backscatter signal energy. The 50 MHz and 90 MHz contrasts were also affected by this increased backscatter since the slope of the contrast versus beam attenuation coefficient increased relative to the data in Figure 3. However, the results from the target range measurements with an 0.2m transmitter-receiver separation (plotted in Figure 6) showed that although the 10 MHz range error increased due to the increased backscatter signal, the 50MHz and 90 MHz target range measurements were unaffected and the range error remained less than 0.1m.

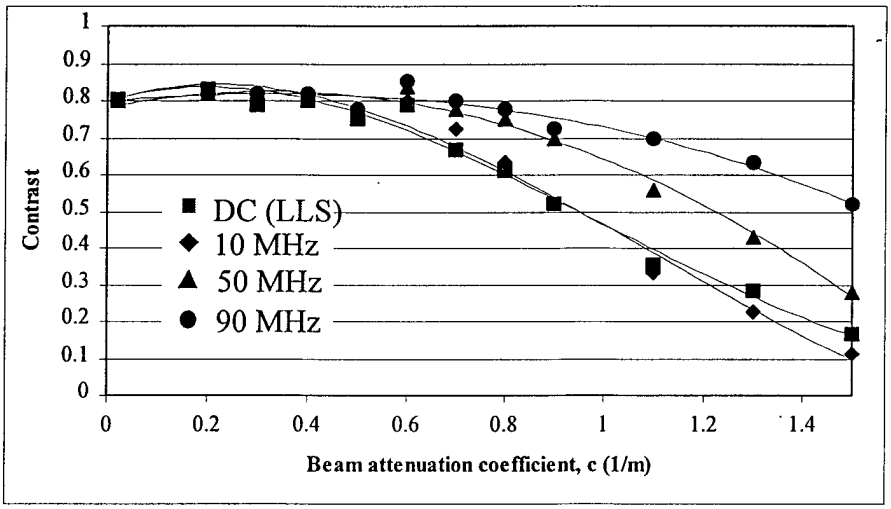

Figure 5. Target contrast measured as a function of beam attenuation coefficient and modulation frequency for a transmitter-receiver separation of 0.2m.

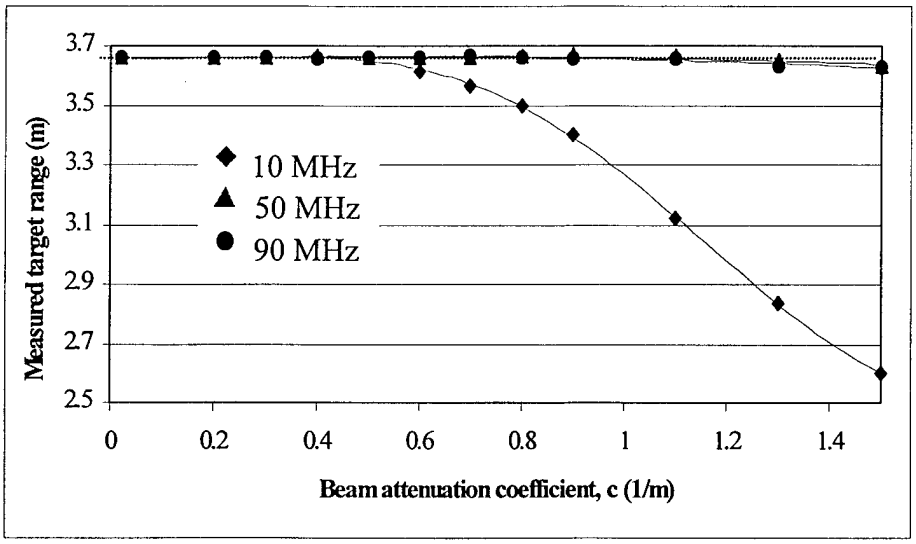

Figure 6. Measured target range as a function of beam attenuation coefficient for each modulation frequency. The transmitter-receiver separation was decreased to 0.2m.

The final set of experiments was completed to study the effect of increasing solar ambient levels on the modulated and unmodulated system performance. As described in the experimental setup, the solar background radiation was simulated by two 500W halogen lights. The light intensity was varied in four levels – both off (DC), both on (DCL3), and two levels in between (DCL1 and DCL2). The DC and AC signal levels were recorded for each 'sun' intensity level. The results for target

contrast at a transmitter-receiver separation of 0.43m are shown in Figure 7. Since the detector remained in the linear operating regime throughout the range of experiments, the modulated signal contrast remained the same for all the 'sun' levels tested and for all three modulation frequencies. However, the DC contrast decreased as the solar background level increased and as the water clarity decreased. The same measurements were taken for a transmitter-receiver separation of 0.2m (see Figure 8). Again, the contrast remained the same for all of the modulated signals but decreased in the unmodulated signals. These results show that all three modulation frequencies are equally effective in rejecting solar ambient noise.

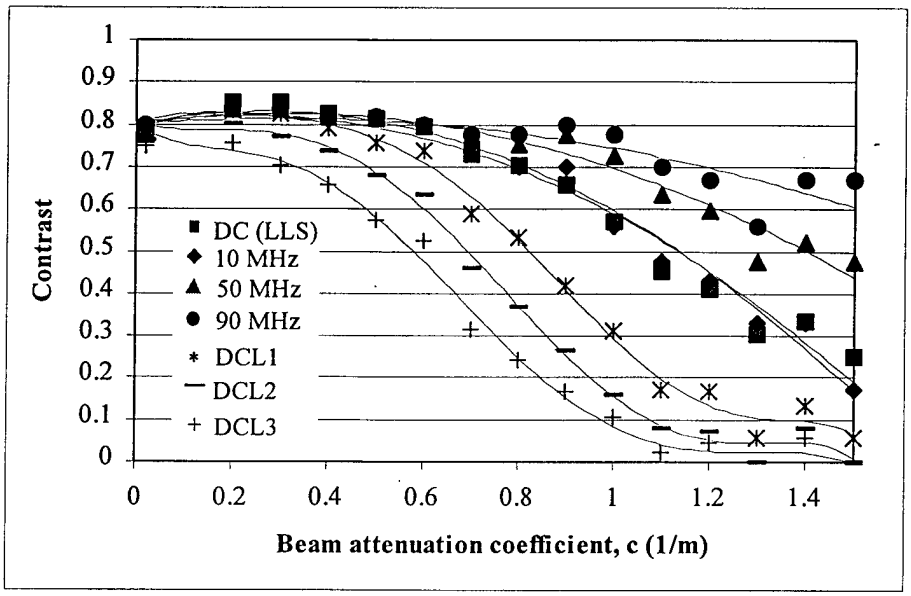

Figure 7. Target contrast as a function of increasing 'solar' background levels for a transmitter-receiver separation of 0.43m. The DC contrasts are shown for four levels of sun intensity (DC, DCL1, DCL2, DCL3). The modulated signal contrasts remained the same over the background light levels tested while the DC contrast decreased as the solar background levels increased.

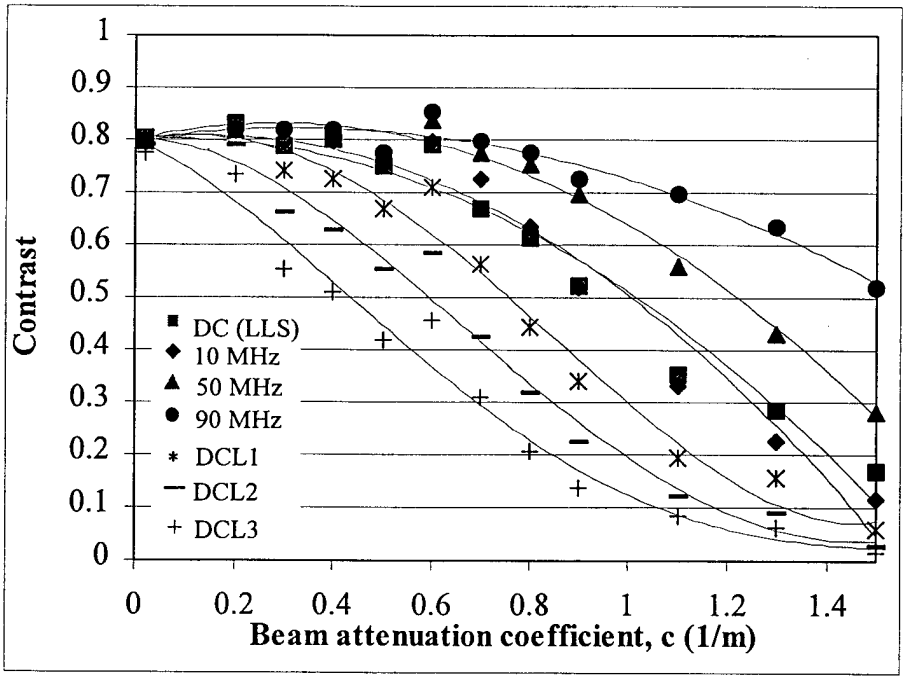

Figure 8. DC and modulated signal contrasts for increasing 'solar' background levels at a transmitter –receiver separation of 0.2m. The DC contrast begins to degrade at lower c values than the corresponding data in Figure 7.

5. SUMMARY

Three sets of experiments were performed with a nonscanning modulated LLS prototype. First, the contrast and phase of a white diffuse target was measured as a function of water clarity and modulation frequency with a transmitter-receiver separation of 0.43m. The 10 MHz data showed no improvement in target contrast over the DC data. However, as the modulation wavelength decreased relative to the transmitter-receiver interaction length, target contrast improved due to backscatter demodulation. The calculations of target range from modulation phase measurements showed that while the 10MHz range data was adversely affected by the backscatter signal, the 50MHz and 90MHz data provided an accurate estimation of target range within 0.1 m for all water clarities. When the transmitter and receiver were moved closer together, the target range measurements for the 50MHz and 90MHz data remained accurate although the absolute target contrast values decreased. However, the 50MHz and 90MHz data still showed improved contrast relative to the DC and 10MHz data. This indicates that the EOID sensor size can be reduced when the hybrid technology is implemented. Although a clear preference for the higher modulation frequencies existed for improving target contrast, all modulation frequencies were shown to reject solar background noise. From these results, it is evident that both the amplitude and phase information contained in a modulated optical signal provides a unique way of improving LLS performance by rejecting scattered light and enhancing target contrast. In the future, the modulated LLS prototype will be fielded in a turbid water environment (i.e., the Chesapeake Bay). The laboratory and field test results will be used to optimize the transition from the modulated LLS prototype to the EOID sensor.

ACKNOWLEDGEMENTS

This work was funded by Dr. Steven Ackleson at the Office of Naval Research (reference #N0001499AF00002).

REFERENCES

1. M. P. Strand, "Underwater electro-optical system for mine identification," *Proc. SPIE, Dectection Technologies for Mines and Minelike Targets,* Vol. 2496, , pp. 487-497, June, 1995.
2. M. P. Strand, B. W, Coles, A. J. Nevis, R. F. Regan, "Laser line-scan fluorescence and multispectral imaging of coral reef environments," *Proc. SPIE, Ocean Optics XIII,* Vol. 2963, pp. 790-795, February, 1997.
3. L. Mullen, P. R. Herczfeld, V. M. Contarino, "Progress in Hybrid Lidar-Radar for Ocean Exploration," *Sea Technology*, Vol. 37, no. 3, pp. 45-52, March, 1996.
4. L. Mullen, V. M. Contarino, P. R. Herczfeld, "Hybrid Lidar-Radar Ocean Experiment," IEEE Transactions on Microwave Theory and Techniques, Vol. 44, no. 12, pp. 2703-2710, December, 1996.
5. S. Q. Duntley, "Underwater lighting by submerged lasers and incandescent sources," Tech. Rep. 71-1 (Scripps Institute of Oceanography, University of California, San Diego, CA), 1971.
6. L. Mullen, V. M. Contarino, A. Laux, B. Concannon, J. Davis, "Modulated Laser Measurements in Simulated Ocean Water," *Proceedings of Ocean Optics XIV*, Kona-Kailua, Hawaii, November, 1998.